Ancient genomic variation underlies repeated ecological adaptation in young stickleback populations

Thomas C. Nelson[1,2,*] and William A. Cresko[1,†]

[1]Institute of Ecology and Evolution, University of Oregon, Eugene, OR 97403
[2]Current address: Division of Biological Sciences, University of Montana, Missoula, MT 59812
*thom.nelson@mso.umt.edu
[†]To whom correspondence should be addressed: wcresko@uoregon.edu

Running title: Ancient genomic variation fuels recent adaptation
Keywords: adaptation, evolutionary genomics, speciation islands, RAD-seq
Abstract word count: 254
Total word count: 5867

ABSTRACT

Adaptation in the wild often involves standing genetic variation (SGV), which allows rapid responses to selection on ecological timescales. However, we still know little about how the evolutionary histories and genomic distributions of SGV influence local adaptation in natural populations. Here, we address this knowledge gap using the threespine stickleback fish (*Gasterosteus aculeatus*) as a model. We extend the popular restriction site-associated DNA sequencing (RAD-seq) method to produce phased haplotypes approaching 700 base pairs (bp) in length at each of over 50,000 loci across the stickleback genome. Parallel adaptation in two geographically isolated freshwater pond populations consistently involved fixation of haplotypes that are identical-by-descent. In these same genomic regions, sequence divergence between marine and freshwater stickleback, as measured by d_{XY}, reaches ten-fold higher than background levels and structures genomic variation into distinct marine and freshwater haplogroups. By combining this dataset with a *de novo* genome assembly of a related species, the ninespine stickleback (*Pungitius pungitius*), we find that this habitat-associated divergent variation averages six million years old, nearly twice the genome-wide average. The genomic variation that is involved in recent and rapid local adaptation in stickleback has actually been evolving throughout the 15-million-year history since the two species lineages split. This long history of genomic divergence has maintained large genomic regions of ancient ancestry that include multiple chromosomal inversions and extensive linked variation. These discoveries of ancient genetic variation spread broadly across the genome in stickleback demonstrate how selection on ecological timescales is a result of genome evolution over geological timescales, and *vice versa*.

IMPACT STATEMENT

Adaptation to changing environments requires a source of genetic variation. When environments change quickly, species often rely on variation that is already present – so-called standing genetic variation – because new adaptive mutations are just too rare. The threespine stickleback, a small fish species living throughout the

Northern Hemisphere, is well-known for its ability to rapidly adapt to new environments. Populations living in coastal oceans are heavily armored with bony plates and spines that protect them from predators. These marine populations have repeatedly invaded and adapted to freshwater environments, losing much of their armor and changing in shape, size, color, and behavior.

Adaptation to freshwater environments can occur in mere decades and probably involves lots of standing genetic variation. Indeed, one of the clearest examples we have of adaptation from standing genetic variation comes from a gene, *eda*, that controls the shifts in armor plating. This discovery involved two surprises that continue to shape our understanding of the genetics of adaptation. First, freshwater stickleback from across the Northern Hemisphere share the same version, or allele, of this gene. Second, the 'marine' and 'freshwater' alleles arose millions of years ago, even though the freshwater populations studied arose much more recently. While it has been hypothesized that other genes in the stickleback genome may share these patterns, large-scale surveys of genomic variation have been unable to test this prediction directly.

Here, we use new sequencing technologies to survey DNA sequence variation across the stickleback genome for patterns like those at the *eda* gene. We find that *every* region of the genome associated with marine-freshwater genetic differences shares this pattern to some degree. Moreover, many of these regions are as old or older than *eda*, stretching back over 10 million years in the past and perhaps even predating the species we now call the threespine stickleback. We conclude that natural selection has maintained this variation over geological timescales and that the same alleles we observe in freshwater stickleback today are the same as those under selection in ancient, now-extinct freshwater habitats. Our findings highlight the need to understand evolution on macroevolutionary timescales to understand and predict adaptation happening in the present day.

INTRODUCTION

The mode and tempo of adaptive evolution depend on the sources of genetic variation affecting fitness (Wright 1932; Orr 2005). While new mutation is the ultimate origin of all genetic variation, recent studies of adaptation in the wild have documented adaptive genetic variation that was either segregating in the ancestral population as standing genetic variation (SGV)(Barrett & Schluter 2008; Domingues *et al.* 2012; Schrider & Kern 2017), or introgressed from a separate population or species (Huerta-Sánchez *et al.* 2014; Fontaine *et al.* 2015). The use of SGV during evolution appears particularly important when dramatic responses to selection occur on ecological timescales, in dozens of generations or fewer (Barrett & Schluter 2008). When environments change rapidly, SGV can propel rapid evolution in ecologically relevant traits even in populations of long-lived organisms like Darwin's finches (Grant & Grant 2002), monkeyflowers (Wright *et al.* 2013), and threespine stickleback fish (Colosimo *et al.* 2005).

The contribution of SGV to rapid divergence has important consequences for our understanding of evolutionary genetics. Existing genetic variants have evolutionary histories that are often unknown, but which may none-the-less have significant impacts on subsequent adaptation (Kirkpatrick & Barton 2006; Wright *et al.* 2013). The abundance, genomic distribution, and fitness effects (Charlesworth *et al.* 1993; Colosimo *et al.* 2005; Kirkpatrick & Barton 2006; Linnen *et al.* 2009; Stankowski & Streisfeld 2015) of SGV are themselves the products of evolution, and their unknown history raises fascinating questions for the genetics of adaptation in the wild. When did adaptive variants originally arise? How are they structured, across both geography and the genome? Which evolutionary forces shaped their current distribution and how might this evolutionary history channel future evolutionary change?

Answers to these questions are critical for our understanding of the importance of SGV in nature, as well as our ability to predict the paths available to adaptation on ecological timescales (Wright *et al.* 2013). Biologists are beginning to probe evolutionary histories of SGV using genome-wide sequence variation across multiple individuals in numerous populations (Pease *et al.* 2016), but this level of inference has

been unavailable for most natural systems because of methodological limitations that remove phase information (e.g. pool-seq: Schlotterer *et al.* 2014) or produce very short reads (e.g. RAD-seq: Davey *et al.* 2011). Here, we investigate the structure and evolutionary history of divergent SGV by modifying the original sheared RAD-seq method to generate ~700 bp haplotypes at tens of thousands of loci sampled across the stickleback genome. This approach allows us to accurately measure sequence variation and estimate divergence times across the genome. By collecting more detailed sequence information at each RAD locus, this approach also provides more accurate estimates of polymorphism and divergence at each locus, and with far smaller sample sizes, compared to traditional short-read methods (Nei 1987 chapters 10 and 13; Wakeley 2009; Cruickshank & Hahn 2014).

SGV has long been postulated to be critical to adaptation in stickleback, and several recent population genomic studies have supported this hypothesis (Hohenlohe *et al.* 2010; Jones *et al.* 2012; Roesti *et al.* 2015; Samuk *et al.* 2017). Marine stickleback have repeatedly colonized freshwater lakes and streams (Bell & Foster 1994b; Jones *et al.* 2012; Wund *et al.* 2016), and adaptive divergence in isolated freshwater habitats is highly parallel at the phenotypic (Colosimo *et al.* 2004; Cresko *et al.* 2004a) and genomic levels (Hohenlohe *et al.* 2010; Jones *et al.* 2012; but see Stuart *et al.* 2017). In addition, analyses of haplotype variation at the genes *eda* (Colosimo *et al.* 2005; Roesti *et al.* 2014) and *atp1a1* (Roesti *et al.* 2014) present two clear results: separate freshwater populations share common 'freshwater' haplotypes that are identical-by-descent (IBD), and sequence divergence between the major marine and freshwater haplogroups suggests their ancient origins – perhaps over two million years ago in the case of *eda* (Colosimo *et al.* 2005). While intriguing, it is not clear whether the deep evolutionary histories of these loci are outliers or representative of more widespread ancient history across the genome. Furthermore, although recent population genomic studies have made important contributions to identifying that SGV across the genome, the short reads employed limit the accuracy of genealogical inference across the genome.

To address fundamental questions of genealogical relationships and molecular evolution in stickleback, we utilize the new RAD-seq haplotyping approach to assay genome-wide variation associated with adaptive divergence in two young freshwater ponds, which formed during the end-Pleistocene glacial retreat (c. 12,000 years ago: Francis *et al.* 1986; Cresko *et al.* 2004a, Fig. 1). In addition, we generated a *de novo* genome assembly of the sister taxon ninespine stickleback (*Pungitius pungitius*), allowing us to estimate divergence times for genealogies across the genome. Our results clearly demonstrate that the previous findings of deep evolutionary history based upon candidate loci are not unique but in fact the rule. A suite of adaptive variation structured into distinct marine and freshwater haplotypes that evolved over millions of years forms the foundation of a deep pool of SGV that undergirds repeated and rapid evolution in stickleback.

METHODS

Sample collection

Wild threespine stickleback were collected from Rabbit Slough (N 61.5595, W 149.2583), Boot Lake (N 61.7167, W 149.1167), and Bear Paw Lake (N 61.6139, W 149.7539). Rabbit Slough is an offshoot of the Knik Arm of Cook Inlet and is known to be populated by anadromous populations of stickleback that are stereotypically oceanic in phenotype and genotype (Cresko *et al.* 2004b; Hohenlohe *et al.* 2010). Boot Lake and Bear Paw Lake are both shallow lakes formed during the end-Pleistocene glacial retreat. Fish were collected in the summers of 2009 (Rabbit Slough), 2010 (Bear Paw Lake), and 2014 (Boot Lake) using wire minnow traps and euthanized *in situ* with Tricaine solution. Euthanized fish were immediately fixed in 95% ethanol and shipped to the Cresko Laboratory at the University of Oregon (Eugene, OR, USA). DNA was extracted from fin clips preserved in 95% ethanol using either Qiagen DNeasy spin column extraction kits or Ampure magnetic beads (Beckman Coulter, Inc) following manufacturer's instructions. Yields averaged 1-2 µg DNA per extraction (~30 mg tissue). Treatment of animals followed protocols approved the University of Oregon Institutional Animal Care and Use Committee (IACUC).

166

167 *Sequencing strategy and rationale*

168 We designed our sequencing to maximize detection of sequence variation and
169 divergence, with the ultimate goal being the estimation of absolute divergence times of
170 marine and freshwater haplogroups. Previous work by us and others using short
171 sequence reads provided clear evidence of changes in relative frequencies of alleles
172 across stickleback populations (Hohenlohe *et al.* 2010; Roesti *et al.* 2014; Lescak *et al.*
173 2015; Roesti *et al.* 2015), but could not sufficiently address questions of haplotype ages.
174 We therefore designed a RAD sequencing approach to (1) accurately estimate
175 sequence diversity within and divergence between threespine stickleback ecotypes and
176 (2) recover sufficient RAD loci that map unambiguously to an outgroup genome
177 sequence from the ninespine stickleback that we could confidently compare diversity
178 within threespine stickleback to divergence from the ninespine stickleback.

179 To achieve our aims, we designed a sequencing method to produce phased
180 haplotypes of ~700 bp at each RAD locus (Fig. 1B-D) and to sample the genome
181 densely enough to identify signatures of selection after the likely dropout of RAD loci
182 without clear homology in the ninespine stickleback genome. We used the single-digest,
183 sheared RAD approach to limit biases in our estimates of sequence diversity. RAD-seq
184 has known biases due to mutations in restriction sites causing allele dropout (Arnold *et*
185 *al.* 2013; Gautier *et al.* 2013), the potential for which increases with increasing
186 sequence divergence and leads to underestimates of genetic diversity. Diversity
187 estimates are, however, substantially more accurate with sheared RAD-seq compared
188 to other RAD-seq approaches (e.g. double-digest RAD-seq: Peterson *et al.* 2012).
189 Importantly for the coalescent analyses we present here, such allele dropout is unlikely
190 to affect estimates of overall divergence across the clade of alleles. When in the rare
191 cases it does, the bias is toward *underestimation* of the divergence age (Arnold *et al.*
192 2013), which would make our findings of deep divergence even more striking.

193 Our sequencing design facilitated accurate inference of sequence variation even
194 with smaller population samples than are typical among population genomic studies.
195 While allele frequency-based statistics like F_{ST} have particularly high variance with small

196 sample sizes (Willing *et al.* 2012), our study is fortunate to be built upon numerous
197 properly powered, previous population genomic studies in stickleback including in these
198 populations. The genome-wide patterns of F_{ST} we observed using our new approach
199 closely matched multiple previous studies (Hohenlohe *et al.* 2010; Jones *et al.* 2012,
200 Fig. 2A). Because of this extensive body of previous work, we relied on F_{ST} only to draw
201 inference of larger genomic regions containing tens or hundreds of RAD loci. Instead,
202 as stated above the focus of this work is to extend these previous findings by
203 addressing the ages of allelic divergence. We therefore do not expect the higher
204 variance associated with smaller sample size to qualitatively influence our results.
205 Importantly, estimation of sequence diversity (π) (Nei 1987) and divergence (d_{XY}) (Nei
206 1987; Cruickshank & Hahn 2014) at a given locus improves greatly with increases in
207 sequence length. Using equations 10.9 and 13.83 from Nei (1987; Box 1 in Cruickshank
208 & Hahn 2014), the predicted sampling variances in both π and d_{XY} using 700 bp
209 sequences in five individuals are lower than those obtained using standard 100 bp
210 sequences at any sample size (Suppl. Fig. S1). Therefore, not only is this novel
211 application of RAD-seq ideally suited for our questions, our findings show that this
212 approach may significantly decrease the necessary sample size, and thus resource
213 expenditure, for many population genomic studies.
214
215 *Library preparation*
216 To identify sufficient sequence variation at a RAD locus, and to simplify
217 downstream sequence processing and analysis, we took advantage of longer
218 sequencing reads available on newer Illumina platforms and the phase information
219 captured by paired-end sequencing. We generated RAD libraries from these samples
220 using the single-digest sheared RAD protocol from Baird et al. (2008) with the following
221 specifications and adjustments: 1 µg of genomic DNA per fish was digested with the
222 restriction enzyme *PstI-HF* (New England Biolabs), followed by ligation to P1 Illumina
223 adaptors with 6 bp inline barcodes. Ligated samples were multiplexed and sheared by
224 sonication in a Bioruptor (Diagenode). To ensure that most of our paired-end reads
225 would overlap unambiguously and produce longer contiguous sequences, we selected a

narrow fragment size range of 425-475 bp. The remainder of the protocol was per Baird et al. (Baird *et al.* 2008b). All fish were sequenced on an Illumina HiSeq 2500 using paired-end 250 bp sequencing reads at the University of Oregon's Genomics and Cell Characterization Core Facility (GC3F).

Sequence processing

Raw Illumina sequence reads were demultiplexed, cleaned, and processed primarily using the Stacks v1.46 pipeline (Catchen *et al.* 2011; Catchen *et al.* 2013a). Paired-end reads were demultiplexed with **`process_shortreads`** and cleaned using **`process_radtags`** using default criteria (throughout this document, names of scripts, programs, functions, and command-line arguments will appear in **`fixed-width font`**). Overlapping read pairs were then merged with **`fastq-join`** (Aronesty 2011). Pairs that failed to merge were removed from further analysis. To retain the majority of the sequence data for analysis in Stacks and still maintain adequate contig lengths, merged contigs were trimmed to 350 bp and all contigs shorter than 350 bp were discarded. We aligned these contigs to the stickleback reference genome (Jones *et al.* 2012; Glazer *et al.* 2015) using **`bbmap`** v35.69 with the most sensitive alignment settings ('**`vslow=t`**'; http://jgi.doe.gov/data-and-tools/bbtools/) and required that contigs mapped uniquely to the reference. We then used the **`pstacks`**, **`cstacks`**, and **`sstacks`** components of the Stacks pipeline to identify RAD-tags and call SNPs using the maximum likelihood algorithm implemented in **`pstacks`**, create a catalog of RAD tags across individuals, and match tags across individuals. All data were then passed through the Stacks error correction module **`rxstacks`** to prune unlikely haplotypes. We ran the Stacks component program **`populations`** on the final dataset to filter loci genotyped in fewer than four individuals in each population and to create output files for sequence analysis. We use the naming conventions of Baird et al. (2008a): A "RAD tag" refers to sequence generated from a single end of a restriction site and the pair of RAD tags sequenced at a restriction site comprises a "RAD locus" (Fig. 1D).

We used the program **phase** v2.1 (Stephens *et al.* 2001; Stephens & Scheet 2005) to phase pairs of RAD tags originating from the same restriction site. We coded haplotypes present at each RAD tag, which often contain multiple SNPs, into multiallelic genotypes. This both simplified and reduced computing time for the phasing process. We also performed coalescent simulations to generate, 'cut', and re-phase haplotypes to demonstrate the high accuracy of this method using sequences and sample sizes similar to those in this study (Suppl. Fig. S2). Custom Python scripts automated this process and are included as supplementary files. We required that each individual had at least one sequenced haplotype at each tag for phasing to be attempted. If a sample had called genotypes at only one tag in the pair, the sample was removed from further analysis of that locus. The resultant phased haplotypes were used to generate sequence alignments for import into BEAST.

We recovered a total of 236,787 RAD tags after filtering, mapping to 151,813 *PstI* restriction sites. At 84,974 restriction sites, we recovered and successfully phased adjacent RAD tags (169,948 RAD tags) into single RAD loci. RAD tags with no variable sites were simply concatenated to the adjacent tag to form a single locus. We retained these 84,974 RAD loci for our analysis. For population genetic analyses, inclusion of singleton (i.e. unpaired) RAD tags did not qualitatively change our results. We chose to restrict genealogical analyses to loci of uniform length and to use the same set of loci in analyses of polymorphism and gene tree topologies.

Ninespine stickleback genome assembly

In order to estimate the T_{MRCA} of threespine stickleback RAD alleles, we used the ninespine stickleback (*Pungitius pungitius*) as an outgroup. RAD sequence analysis, however, relies on the presence of homologous restriction sites among sampled individuals and results in null alleles when mutations occur within a restriction site(Arnold *et al.* 2013). Because this probability increases with greater evolutionary distance among sampled sequences, we elected to use RAD-seq to only estimate sequence variation within the threespine stickleback. We then generated a contig-level *de novo* ninespine stickleback genome assembly from a single ninespine stickleback

individual from St. Lawrence Island, Alaska (collected by J. Postlethwait) using DISCOVAR *de novo* revision 52488 (https://software.broadinstitute.org/software/discovar/blog/). We used this single ninespine stickleback haplotype to estimate threespine-ninespine sequence divergence and time calibrate coalescence times within the threespine stickleback. DISCOVAR de novo requires a single shotgun library of paired-end 250-bp sequence reads from short-insert-length DNA fragments. High molecular weight genomic DNA was extracted from an ethanol-preserved fin clip by proteinase K digestion followed by DNA extraction with Ampure magnetic beads. Purified genomic DNA was mechanically sheared by sonication and size selected to a range of 200-800 bp by gel electrophoresis and extraction. We selected this fragment range to agree with the recommendations for *de novo* assembly using DISCOVAR *de novo*. This library was sequenced on a single lane of an Illumina HiSeq2500 at the University of Oregon's Genomics and Cell Characterization Core Facility (GC3F: https://gc3f.uoregon.edu/). We assembled the draft ninespine stickleback genome using DISCOVAR de novo. Raw sequence read pairs were first quality filtered and adaptor sequence contamination removed using the program **process_shortreads**, which is included in the Stacks analysis pipeline (Catchen *et al.* 2013b). We ran the genome assembly on the University of Oregon's Applied Computational Instrument for Scientific Synthesis (ACISS: http://aciss-computing.uoregon.edu).

Alignment of RAD tags to the ninespine assembly

We included the single ninespine stickleback haplotype into our sequence analyses by aligning a single phased threespine stickleback RAD haplotype from each locus to the ninespine genome assembly. For those that aligned uniquely (59,254 RAD loci), we used a custom Python script to parse the alignment fields of the output BAM file (Li *et al.* 2009) and reconstruct the ninespine haplotype by introducing threespine-ninespine substitutions into the threespine RAD locus sequence. The final dataset consists of 57,992 RAD loci that mapped to the 21 threespine stickleback chromosomes and aligned uniquely to the ninespine assembly.

Lineage sorting and time to the most recent common ancestor

Allelic divergence can occur by multiple modes of lineage sorting during adaptation. To identify patterns of lineage sorting associated with freshwater colonization, we analyzed gene tree topologies at all RAD loci using BEAST v. 1.7 (Drummond & Rambaut 2007; Drummond *et al.* 2012). We chose BEAST because it co-estimates tree topologies and node ages for sequenced genomic loci. BEAST does not explicitly perform model selection, and this may affect divergence time estimates in genomic regions under direct or indirect selection. However, other methods developed to estimate the age of adaptive alleles model evolutionary scenarios that are likely not relevant to the evolutionary histories we infer here. First, some models assume a recent origin of an adaptive allele compared to adjacent genomic variation (Peter *et al.* 2012; Ormond *et al.* 2016), which is the opposite of what we describe here, so that measures of variation at linked sites and the decay of linkage disequilibrium can be used to estimate when a sweep began. Selection in the stickleback populations we study likely acted on SGV, as has been supported by previous studies, and we hypothesize that this SGV may be quite old. Therefore, adaptive alleles already existed on distinct haplotype backgrounds, which masks the differences between selected and linked neutral sites.

Second, a recent model developed to infer ages of standing genetic variants assumes that the variant was evolving neutrally at some point during its trajectory through a population (Peter *et al.* 2012). This assumption is unlikely for many of the loci we detect here, except in the very distant past and for those loci that have evolved recently arose in genomic regions already heavily influenced by selection. Rather, the patterns of haplotype variation we observed in the genomic regions that differentiate marine and freshwater populations reflect long-term maintenance and isolation of separate haplogroups that mimics population structure and even speciation, with selective sweeps being important but constituting a small minority of the time these haplotypes have segregating in the stickleback metapopulation. For all of these reasons we therefore chose to estimate tree topologies and divergence times with BEAST, which makes minimal assumptions regarding specific evolutionary processes.

We used blanket parameters and priors for BEAST analyses across all RAD loci. Markov chain Monte Carlo (MCMC) runs of 1,000,000 states were specified, and trees logged every 100 states. We used a coalescent tree prior and the GTR+Γ substitution model with four rate categories and uniform priors for all substitution rates. We identified evidence of lineage sorting by using the program **`treeannotator`** v1.7.5 to select the maximum clade credibility (MCC) tree for each RAD locus and the **`is.monophyletic()`** function included in the R package 'ape' v3.0 (Paradis *et al.* 2004; Popescu *et al.* 2012). We determined for each MCC tree whether tips originating from marine (RS) or freshwater (BL+BP) formed monophyletic clades.

To convert node ages estimated in BEAST into divergence times, in years, we assumed a 15 million-year divergence time between threespine and ninespine stickleback at each RAD locus (Aldenhoven *et al.* 2010). The T_{MRCA} of all alleles in each gene tree was set at 15 Mya and each node age of interest was converted into years relative to the total height of the tree. Additionally, to use the ninespine stickleback as an outgroup, we required that threespine stickleback haplotypes at a RAD locus were monophyletic to the exclusion of the ninespine haplotype. Doing so reduced our analysis to 49,672 RAD loci for analyses included in Fig. 4 of the main text. RAD loci not showing this pattern of lineage sorting did not show evidence of a genome-wide correlation with marine-freshwater divergence and thus do not impact the assertions in the main text. We used medians of the posterior distributions as point estimates of T_{MRCA} for each RAD locus. Because of the somewhat limited information from any single RAD locus, and because the facts of the genealogical process mean that the true T_{MRCA} at any locus likely differs from the 15 My estimate (Kingman 1982a, b; Tajima 1983), we do not rely heavily on T_{MRCA} estimates at individual RAD loci. Rather, we use these estimates to understand patterns of broad patterns of ancestry throughout the threespine stickleback genome — spatially along chromosomes and genome-wide patterns.

We determined T_{MRCA} outlier genomic regions by permuting and kernel smoothing the genomic distribution of T_{MRCA} estimates using the same window sizes as we present in the main text. Windows where the actual T_{MRCA} exceeded 99.9% of

374 permuted windows were considered outliers. This method controls for the local density
375 of RAD loci (poorly sampled regions will have larger confidence bands) and the size of
376 the windows used.
377
378 *Sequence diversity and haplotype networks*
379 We quantified sequence diversity within and among populations and sequence
380 divergence between populations using R v3 (R Core Team 2016). We used the R
381 package 'ape' (Paradis *et al.* 2004) to compute pairwise distance matrices for all alleles
382 at each RAD locus and used these matrices to calculate the average pairwise
383 nucleotide distances, π, within and among populations along with d_{XY}, the average
384 pairwise distance between two sequences using only across-population comparisons
385 (Nei 1987). We also calculated the haplotype-based F_{ST} from Hudson et al. (1992)
386 implemented in the R package 'PopGenome' v2.2.4 (Pfeifer *et al.* 2014). We used
387 permutation tests written in R to identify differences in variation within- and between-
388 habitat type at divergent RAD loci versus the genome-wide distributions. Mann-Whitney-
389 Wilcoxon tests implemented in R were used to identify variation in genome-wide
390 diversity among populations and habitat types.
391 We constructed haplotype networks of the RAD loci at *eda* and *atp1a1* using the
392 infinite sites model with the function **`haploNet()`** in the R package 'pegas' (Paradis
393 2010). The *atp1a1* network was constructed from from a RAD locus spanning exon 15
394 of *atp1a1* and including portions of introns 14 and 15 at (chr1:21,726,729-21,727,381
395 [BROAD S1, v89]; chr1: 26,258,117-26,257,465 [re-scaffolding from Glazer, *et al*
396 (2015)]). The *eda* network spans exon 2 and portions of introns 1 and 3 of *eda* (chr4:
397 12,808,396-12,809,030).
398
399 *Code availability*
400 Scripts used to phase RAD-tags, summarize gene trees, calculate population genetic
401 statistics, and produce figures and statistics presented in paper are available at
402 https://github.com/thomnelson/ancient-divergence. Scripts for processing raw sequence
403 data are available from the authors upon request.

Data availability

Raw sequence data supporting these findings are available on the Sequence Read Archive at PRJNAXXXXXX. The final datasets needed to reproduce the figures and statistics presented in the paper are available at https://github.com/thomnelson/ancient-divergence.

RESULTS AND DISCUSSION

Parallel adaptation to freshwater environments has been a major theme of stickleback evolutionary history (Bell & Foster 1994a). Stereotypical morphological changes to, for example, bony armor(Colosimo *et al.* 2004) and craniofacial structures (Kimmel *et al.* 2005) presumably reflect adaptation to similar selective regimes (Reimchen 1994; Arnegard *et al.* 2014). These phenotypic changes are accompanied by parallel genomic divergence (Hohenlohe *et al.* 2010; Jones *et al.* 2012), which involves large regions spanning many megabases (Schluter & Conte 2009; Roesti *et al.* 2014), including multiple chromosomal inversions (Jones *et al.* 2012). The leading hypothesis for the genetics of parallel divergence in stickleback posits that distinct freshwater-adaptive haplotypes that are identical-by-descent (IBD) are shared among freshwater populations due to historical gene flow between marine and freshwater populations (Schluter & Conte 2009). We tested for the presence of these haplotypes directly and at a genomic scale.

Parallel divergence involves a shared suite of haplotypes genome-wide

Our sequencing strategy produced 57,992 RAD loci, with 690 potential variable sites each, present across the three threespine stickleback populations and aligned to the ninespine stickleback genome assembly. These data comprise over 40 Mb of sequence, or nearly 10% of the threespine stickleback genome (9.5% of 419 Mb assigned to chromosomes) (Jones *et al.* 2012; Glazer *et al.* 2015). All loci we recovered were polymorphic and we observed a median of seven segregating sites per locus

(range: 2-155, Suppl. Fig. S3, Suppl. Table 1). By including haplotypes from all three populations in these genealogical analyses, we were able to jointly calculate population genetic statistics (F_{ST}, π, d_{XY}) and identify patterns of identity-by-descent (IBD) among populations, which we defined as haplotypes from two populations forming a monophyletic group to the exclusion of the third population.

We find that parallel population genomic divergence in the two freshwater pond populations consistently involved haplotypes that were identical-by-descent (IBD) among both freshwater populations (Fig. 2). Background F_{ST} between populations ranged from 0.139-0.226, with genome-wide differentiation between the freshwater populations BL and BP being highest ($F_{ST(RS-BL)}$ = 0.139, $F_{ST(RS-BP)}$ = 0.194, $F_{ST(BL-BP)}$ = 0.226; two-sided Mann-Whitney test for all pairwise comparisons: $p \leq 1x10^{-10}$). The degree and genomic distribution of pairwise F_{ST} between the BL, BP, and RS populations were similar to those previously reported (Hohenlohe *et al.* 2010). This similarity included marine-freshwater F_{ST} outlier regions on chromosome 4 over a broad span in which the *eda* gene is embedded (orange triangle in Fig. 2A), and three regions now known to be associated with chromosomal inversions on chromosomes 1, 11, and 21 (yellow bars in Fig. 2; hereafter referred to as *inv1*, *inv11*, and *inv21*). The gene *atp1a1* (green triangle in Fig. 2A) is contained within *inv1*. As expected, we found distinct haplogroups associated with marine and freshwater habitats at both *eda* and *atp1a1* (Fig. 3, insets).

Strikingly, this finding of habitat specific haplogroups was not at all unique to these well studied genes or chromosomal inversions. The two isolated freshwater populations shared IBD haplotypes within all common marine-freshwater F_{ST} peaks even though IBD was rare elsewhere (Fig. 2B). Furthermore, we observed a separate clade of haplotypes representing the marine RS population at the majority (1129 of 2172, 52%) of RAD loci showing freshwater IBD. The result was a genome-wide pattern of reciprocal monophyly between marine and freshwater haplotypes. Notably, this is the same genealogical structure previously reported at *eda* (Colosimo *et al.* 2005; Roesti *et al.* 2014) and *atp1a1* (Roesti *et al.* 2014), demonstrating that these loci are but a small part of a genome-wide suite of genetic variation sharing similar habitat-specific

evolutionary histories, and the previous documentation of their genealogies was a harbinger of a much more extensive pattern across the genome revealed here. Hereafter, we refer collectively to this class of RAD loci as 'divergent loci'.

Adaptive marine-freshwater sequence divergence involves ancient allelic origins

Because the genealogical structure of divergence across the genome mirrors that at *eda* and *atp1a1*, we asked whether levels of sequence variation and divergence also showed consistent genomic patterns. At all RAD loci we therefore calculated π within each population, as well as in the combined freshwater populations, and d_{XY} between marine and freshwater habitat types. Genome-wide diversity was similar across populations and habitat types (mean $\pi_{RS} = 0.0032$, $\pi_{BL} = 0.0034$, $\pi_{BP} = 0.0026$, $\pi_{FW} = 0.0038$) and comparable to previous estimates (Hohenlohe *et al.* 2010). Likewise, genome-wide d_{XY} among habitat types was modest (0.0049) when compared to π across all populations ($\pi = 0.0042$, two-sided Mann-Whitney test: $p \leq 1x10^{-10}$; Suppl. Fig. S4). Among divergent loci, however, we observed reductions in diversity in both habitats (mean $\pi_{RS\text{-divergent}} = 0.0012$, $\pi_{RS\text{-divergent}} = 0.0016$, two-sided permutation test: $p \leq 1x10^{-4}$, Fig. 3), indicating natural selection in both habitats. Sequence divergence associated with reciprocal monophyly was striking, however, averaging nearly three times the genome-wide mean (mean $d_{XY\text{-divergent}} = 0.0124$). This divergence ranged more than an order of magnitude (0.0013–0.0442), from substantially lower than the genome-wide average to ten times greater than the average. These findings indicate that much of the genetic variation underlying adaptive divergence is vastly older than the diverging freshwater populations themselves. Not only was adaptive variation standing and structured by habitat, but it has been segregating and accumulating for millennia.

These data clearly support the hypothesis of Schluter and Conte (2009) of ancient haplotypes 'transported' among freshwater populations. Much of the divergence we observed was ancient in origin, with levels of sequence divergence at some RAD loci exceeding that observed at *eda* (Fig. 3, gold line) and suggestive of divergence times of at least two million years ago (Colosimo *et al.* 2005). Our observation that

494 sequence variation was consistently reduced in both habitat types emphasizes that
495 alternative haplotypes at these loci are likely selected for in the marine population as
496 well as the freshwater. These alternative fitness optima — driven by divergent ecologies
497 — provide a favorable landscape for the maintenance of variation (Charlesworth *et al.*
498 1997; Lenormand 2002), but also lead to a more potent barrier to gene flow among
499 freshwater populations if there are fitness consequences in the marine habitat for
500 stickleback carrying freshwater-adaptive variation. Conditional fitness effects through
501 genetic interactions (i.e. dominance or epistasis: Otto & Bourguet 1999; Phillips 2008)
502 and genotype-by-environment interactions (McGuigan *et al.* 2011) could potentially
503 extend the residence time of freshwater haplotypes in the marine habitat. Future work
504 should consider the phenotypic effects of divergently adaptive variation in different
505 external environments (McGuigan *et al.* 2011; McCairns & Bernatchez 2012).
506 Adaptive divergence between marine and freshwater stickleback genomes is
507 likely ongoing, with recently derived alleles arising on already highly divergent genomic
508 backgrounds. We found reciprocal monophyly associated with a spectrum of sequence
509 divergence, including a substantial fraction of divergent loci (11.0%, 124/1129) with d_{XY}
510 below the genome-wide average. Thus, ongoing marine-freshwater ecological
511 divergence may continue to yield additional marine-freshwater genomic divergence.
512 Moreover, while this younger variation is shared between the freshwater populations in
513 this study, and localizes to genomic regions of divergence shared globally (Jones *et al.*
514 2012), some adaptive variants may be distributed only locally (e.g. limited to southern
515 Alaska or the eastern Pacific basin). Global surveys of shared variation have been
516 performed (Jones *et al.* 2012), but future work in this system should quantify the
517 distributions of locally or regionally limited genomic variation involved in ecological
518 divergence, because regional pools of variation may contribute substantially to
519 stickleback genomic and phenotypic diversity (Stuart *et al.* 2017).
520
521 *Habitat associated genomic divergence is as old as the threespine stickleback species*
522 Sequence divergence provides an important relative, but ultimately incomplete,
523 evolutionary timescale. To more directly compare the timescales of ecological

524 adaptation and genomic evolution, we translated patterns of sequence variation into the
525 time to the most recent common ancestor (T_{MRCA}) of allelic variation, in years. To do so,
526 we performed a *de novo* genome assembly of the ninespine stickleback (*Pungitius*
527 *pungitius*), a member of the Gasterosteidae that diverged from the threespine
528 stickleback lineage approximately 15 million years ago (MYA) (Aldenhoven *et al.* 2010)
529 (Fig. 4A, Suppl. Table 2). We then aligned our RAD dataset to this assembly and
530 estimated gene trees for each alignment with BEAST (Drummond *et al.* 2012), setting
531 divergence to the ninespine stickleback at 15 MYA (see Methods).
532 We find that the divergence of key marine and freshwater haplotypes has been
533 ongoing for millions of years and extends back to the split with the ninespine stickleback
534 lineage (Fig. 4B). Genome-wide variation averaged 4.1 MY old, and T_{MRCA} for the vast
535 majority of RAD loci was under 5 MY old. In contrast, divergence times at habitat-
536 associated loci averaged 6.4 MYA and, amazingly, the most ancient 10% (118 of 1129)
537 are each estimated at over 10 MY old. This deep genomic divergence not only
538 underscores that local adaptation to marine and freshwater habitats has been occurring
539 throughout the history of the threespine stickleback lineage, for which there is evidence
540 in the fossil record going back 10 million years (Bell *et al.* 1985), but it also
541 demonstrates that at least some of the variation fueling those ancient events has
542 persisted until the present day. In some genomic regions, then, marine and freshwater
543 threespine stickleback are as divergent as threespine and ninespine stickleback, which
544 are classified into separate genera.
545 Adaptive divergence has impacted the history of the stickleback genome as a
546 whole (Fig. 4C). We identified 32.6 Mb, or 7.5% of the genome, as having elevated
547 T_{MRCA} (gray boxes in Fig. 4C; two-sided permutation test of smoothed genomic
548 intervals, $p \leq 0.001$). Outside of the non-recombining portion of the sex chromosome
549 (chr. 19), the oldest regions of the stickleback genome were those enriched for
550 divergent loci. Patterns of ancient ancestry closely mirrored recent divergence in allele
551 frequencies (Fig. 2A) and it appears that historical and contemporary marine-freshwater
552 divergence has impacted ancestry across much of the length of some chromosomes.
553 Chromosome 4, for example, contains at least three broad peaks in T_{MRCA} and a total of

554 5.9 Mb identified as genome-wide outliers (two-sided permutation test, $p \leq 0.001$). This
555 chromosome has been of particular interest because of its association with a number of
556 phenotypes (Colosimo *et al.* 2004; Miller *et al.* 2014), including fitness (Barrett *et al.*
557 2008). We found the major-effect armor plate locus *eda* comprised a local peak (mean
558 T_{MRCA} = 6.4 MYA) nested within a large region of deep ancestry spanning 8.1 Mb.
559 Moreover, at least two other peaks distal to *eda,* centered at 21.4 Mb and 26.6 Mb,
560 were also several million years older than the genomic average at 6.8 MYA and 7.0
561 MYA, respectively.
562
563 *Long-term divergence maintains linked variation and promotes genomic structural*
564 *evolution*
565 Intriguingly, genomic regions of elevated T_{MRCA} remained outliers even after
566 removing marine-freshwater relative divergence outlier loci (as measured by F_{ST}: Suppl.
567 Fig. S5). We estimated that 7.5% of the genome had increased T_{MRCA} even though only
568 1.9% of RAD loci (1129 of 57,992) were classified as divergent based on marine-
569 freshwater reciprocal monophyly. When we removed these loci, along with loci with
570 elevated marine-freshwater F_{ST} ($F_{ST} > 0.5$), many of the regions in which they resided
571 were still T_{MRCA} outliers. It is possible that the remainder of this old variation is neutral
572 with respect to fitness. However, we identified divergence outliers based on only a
573 single axis of divergence: the marine-freshwater axis. Throughout the entire species
574 range, populations are locally experiencing multiple axes of divergence, including lake-
575 stream and benthic-limnetic axes (McKinnon & Rundle 2002), that often shares a
576 common genomic architecture (Deagle *et al.* 2012; Roesti *et al.* 2015). Our data may
577 indicate underlying similarities in selection regimes. Alternatively, this co-localized
578 ancient variation may represent the accumulation of adaptive divergence along multiple
579 axes in the same genomic regions, whether or not the underlying adaptive variants are
580 the same. Aspects of the genomic architecture, such as gene density or local
581 recombination rates, may in part govern where in the genome adaptive divergence can
582 occur (Roesti *et al.* 2013; Aeschbacher *et al.* 2017; Samuk *et al.* 2017). Multiple axes of

583 divergence may therefore act synergistically to maintain genomic variation across the
584 stickleback metapopulation.
585 Nevertheless, much of the ancient variation we observe may in fact itself be
586 neutral, having been maintained by close linkage to loci under divergent selection
587 between the marine and freshwater habitats (Charlesworth *et al.* 1997). Indeed, the
588 broadest peaks of T_{MRCA} we observe occur in genomic regions with low rates of
589 recombination (Roesti *et al.* 2013; Glazer *et al.* 2015) in other stickleback populations,
590 which would extend the size of the linked region affected by divergent selection. On
591 ecological timescales, low recombination rates in stickleback are thought to promote
592 divergence by making locally adapted genomic regions resistant to gene flow (Roesti *et*
593 *al.* 2013). Our results potentially extend the inferred impact of recombination rate
594 variation on genomic variation to timescales that are 1000-fold longer, maintaining both
595 multimillion-year-old adaptive variation and large stores of linked genetic variation.
596 Future modeling efforts will be needed to explore the range of population genetic
597 parameter values (e.g. selection coefficients, migration rates, and recombination rates)
598 required to produce the extent of divergence we see here.
599 Lastly, our findings demonstrate that known chromosomal inversions maintain
600 globally distributed, multilocus haplotypes. The three chromosomal inversions known to
601 be associated with marine-freshwater divergence (Jones *et al.* 2012; Roesti *et al.* 2015)
602 (*inv1*, *inv11*, and *inv21*; yellow bars in Fig. 4C) all showed sharp spikes in T_{MRCA}.
603 Genomic signatures of these inversions are distributed throughout the species range,
604 including coastal marine-freshwater population pairs in the Pacific and Atlantic basins
605 (Jones *et al.* 2012) and inland lake-stream pairs in Switzerland (Roesti *et al.* 2015).
606 Despite our limited geographic sampling, our finding that all three of these inversions
607 are over six million years old is further evidence of single, ancient origins of each,
608 followed by their spread across the species range. Each inversion contained a high
609 density of divergent RAD loci (*inv1*: 64% of loci divergent; *inv11*: 60%; *inv21*: 71%) but
610 we also identified regions within these inversions in which haplotypes from marine or
611 freshwater habitats, or both, were not monophyletic. *inv1* and *inv11* both contained two
612 regions separated by loci in which neither habitat type was monophyletic; *inv21*, the

largest of the three, contained ten such regions. Additionally, T_{MRCA} and F_{ST} decreased sharply to background levels outside of the inversions, demonstrating the potential for gene flow and recombination to homogenize variation in these regions. We interpret this as evidence that these inversions help maintain linkage disequilibrium among multiple divergently adaptive variants in regions susceptible to homogenization (Kirkpatrick & Barton 2006; Guerrero *et al.* 2012). The presence of these inversions in addition to divergence in regions of generally low recombination (Glazer *et al.* 2015), therefore, further supports the hypothesis that the recombinational landscape can influence where in the genome adaptive divergence can occur (Roesti *et al.* 2013; Samuk *et al.* 2017) and emphasizes the degree to which gene flow among divergently adapted stickleback populations has impacted global genomic diversity.

Conclusions

Selection operating on two very different timescales — the ecological and the geological — has shaped genomic patterns of SGV in the threespine stickleback. On ecological timescales, selection drives phenotypic divergence in decades or millennia by sorting SGV across geography and throughout the genome (Hendry *et al.* 2002; Hohenlohe *et al.* 2010; Lescak *et al.* 2015; Roesti *et al.* 2015). Our findings show that persistent ecological diversity and continual local adaptation of stickleback has set the stage for long-term divergent selection and for the accumulation and maintenance of adaptive variation over geological timescales. Some of the genetic variants fueling contemporary, rapid adaptation may even have been present – and under selection – since before the threespine-ninespine stickleback lineages split. The genomic architecture of ecological adaptation in one focal population is therefore the product of millions of years of evolution taking place in multiple populations, many of which are now extinct. These findings underscore the need to understand macroevolutionary patterns when studying microevolutionary processes, and vice versa.

643 ACKNOWLEDGEMENTS

644 We thank P. Phillips, M. Streisfeld, J. Postlethwait, K. Sterner for valuable input and
645 lively discussion throughout this project. We also thank K. Alligood, E. Beck, S.
646 Bassham, M. Chase, M. Currey, M. Hahn, L. Fishman, P. Ralph, C. Small, S.
647 Stankowski, J. Willis, two anonymous reviewers, and members of the Cresko Lab and
648 the Institute of Ecology and Evolution for advice and comments on previous versions of
649 this manuscript. J. Postlethwait graciously donated ninespine stickleback tissue,
650 collected under award XXXXXXXX. We acknowledge National Science Foundation
651 awards NSF DEB 1501423 (WAC and TCN), NSF DEB 0949053 (WAC), and National
652 Institutes of Health award NIH T32GM007413 (TCN).

653

654 AUTHOR CONTRIBUTIONS

655 TCN and WAC conceived of the project and designed sampling, sequencing, and
656 analysis. TCN prepared sequencing libraries, wrote software, and performed data
657 analysis. TCN and WAC wrote the paper.

658

659 CONFLICTS OF INTEREST

660 The authors declare no conflicts of interest.

661

662

663 LITERATURE CITED
664
665
666 Aeschbacher, S., Selby, J.P., Willis, J.H. & Coop, G. (2017). Population-genomic inference of
667 the strength and timing of selection against gene flow. *P Natl Acad Sci USA*, 114, 7061-
668 7066.
669 Aldenhoven, J.T., Miller, M.A., Corneli, P.S. & Shapiro, M.D. (2010). Phylogeography of
670 ninespine sticklebacks (Pungitius pungitius) in North America: glacial refugia and the
671 origins of adaptive traits. *Mol Ecol*, 19, 4061-4076.
672 Arnegard, M.E., McGee, M.D., Matthews, B., Marchinko, K.B., Conte, G.L., Kabir, S. *et al.*
673 (2014). Genetics of ecological divergence during speciation. *Nature*, 511, 307-311.
674 Arnold, B., Corbett-Detig, R.B., Hartl, D. & Bomblies, K. (2013). RADseq underestimates
675 diversity and introduces genealogical biases due to nonrandom haplotype sampling. *Mol*
676 *Ecol*, 22, 3179-3190.
677 Aronesty, E. (2011). ea-utils: Command-line tools for processing biological sequencing data.
678 Baird, N.a., Etter, P.D., Atwood, T.S., Currey, M.C., Shiver, A.L., Lewis, Z.a. *et al.* (2008a).
679 Rapid SNP discovery and genetic mapping using sequenced RAD markers. *Plos One*, 3,
680 1-7.
681 Baird, N.A., Etter, P.D., Atwood, T.S., Currey, M.C., Shiver, A.L., Lewis, Z.A. *et al.* (2008b).
682 Rapid SNP discovery and genetic mapping using sequenced RAD markers. *Plos One*, 3,
683 e3376.
684 Barrett, R.D., Rogers, S.M. & Schluter, D. (2008). Natural selection on a major armor gene in
685 threespine stickleback. *Science*, 322, 255-257.
686 Barrett, R.D.H. & Schluter, D. (2008). Adaptation from standing genetic variation. *TREE*, 23, 38-
687 44.
688 Bell, M.A., Baumgartner, J.V. & Olson, E.C. (1985). Patterns of Temporal Change in Single
689 Morphological Characters of a Miocene Stickleback Fish. *Paleobiology*, 11, 258-271.
690 Bell, M.A. & Foster, S.A. (1994a). Evolutionary inference: the value of viewing evolution through
691 stickleback-tinted glasses. In: *The Evolutionary Biology of the Threespine Stickleback*
692 (eds. Bell, MA & Foster, SA). Oxford University Press New York, pp. 472-486.
693 Bell, M.A. & Foster, S.A. (1994b). Introduction to the evolutionary biology of the threespine
694 stickleback. In: *The Evolutionary Biology of the Threespine Stickleback* (eds. Bell, MA &
695 Foster, SA). Oxford University Press New York, pp. 1-27.
696 Catchen, J., Hohenlohe, P.A., Bassham, S., Amores, A. & Cresko, W.A. (2013a). Stacks: an
697 analysis tool set for population genomics. *Mol Ecol*, 22, 3124-3140.
698 Catchen, J., Hohenlohe, P.a., Bassham, S., Amores, A. & Cresko, W.a. (2013b). Stacks: An
699 analysis tool set for population genomics. *Mol Ecol*, 22, 3124-3140.
700 Catchen, J.M., Amores, A., Hohenlohe, P., Cresko, W. & Postlethwait, J.H. (2011). Stacks:
701 building and genotyping Loci de novo from short-read sequences. *G3-Genes Genom*
702 *Genet*, 1, 171-182.
703 Charlesworth, B., Morgan, M.T. & Charlesworth, D. (1993). The Effect of Deleterious Mutations
704 on Neutral Molecular Variation. *Genetics*, 134, 1289-1303.
705 Charlesworth, B., Nordborg, M. & Charlesworth, D. (1997). The effects of local selection,
706 balanced polymorphism and background selection on equilibrium patterns of genetic
707 diversity in subdivided populations. *Genet Res*, 70, 155-174.
708 Colosimo, P.F., Hosemann, K.E., Balabhadra, S., Villarreal, G., Jr., Dickson, M., Grimwood, J.
709 *et al.* (2005). Widespread parallel evolution in sticklebacks by repeated fixation of
710 Ectodysplasin alleles. *Science*, 307, 1928-1933.

711 Colosimo, P.F., Peichel, C.L., Nereng, K., Blackman, B.K., Shapiro, M.D., Schluter, D. *et al.*
712 (2004). The genetic architecture of parallel armor plate reduction in threespine
713 sticklebacks. *PLoS Biol*, 2, 635-641.
714 Cresko, W.A., Amores, A., Wilson, C., Murphy, J., Currey, M., Phillips, P. *et al.* (2004a). Parallel
715 genetic basis for repeated evolution of armor loss in Alaskan threespine stickleback
716 populations. *Proc Natl Acad Sci U S A*, 101, 6050-6055.
717 Cresko, W.a., Amores, A., Wilson, C., Murphy, J., Currey, M., Phillips, P. *et al.* (2004b). Parallel
718 genetic basis for repeated evolution of armor loss in Alaskan threespine stickleback
719 populations. *P Natl Acad Sci USA*, 101, 6050-6055.
720 Cruickshank, T.E. & Hahn, M.W. (2014). Reanalysis suggests that genomic islands of
721 speciation are due to reduced diversity, not reduced gene flow. *Mol Ecol*, 23, 3133-3157.
722 Davey, J.W., Hohenlohe, P.A., Etter, P.D., Boone, J.Q., Catchen, J.M. & Blaxter, M.L. (2011).
723 Genome-wide genetic marker discovery and genotyping using next-generation
724 sequencing. *Nat Rev Genet*, 12, 499-510.
725 Deagle, B.E., Jones, F.C., Chan, Y.F., Absher, D.M., Kingsley, D.M. & Reimchen, T.E. (2012).
726 Population genomics of parallel phenotypic evolution in stickleback across stream-lake
727 ecological transitions. *Proc Roy Soc B-Biol Sci*, 279, 1277-1286.
728 Domingues, V.S., Poh, Y.P., Peterson, B.K., Pennings, P.S., Jensen, J.D. & Hoekstra, H.E.
729 (2012). Evidence of adaptation from ancestral variation in young populations of beach
730 mice. *Evolution*, 66, 3209-3223.
731 Drummond, A.J. & Rambaut, A. (2007). BEAST: Bayesian evolutionary analysis by sampling
732 trees. *BMC Evol Biol*, 7, 214.
733 Drummond, A.J., Suchard, M.A., Xie, D. & Rambaut, A. (2012). Bayesian phylogenetics with
734 BEAUti and the BEAST 1.7. *Mol Biol Evol*, 29, 1969-1973.
735 Fontaine, M.C., Pease, J.B., Steele, A., Waterhouse, R.M., Neafsey, D.E., Sharakhov, I.V. *et al.*
736 (2015). Mosquito genomics. Extensive introgression in a malaria vector species complex
737 revealed by phylogenomics. *Science*, 347, 1258524.
738 Francis, R.C., Baumgartner, J.V., Havens, A.C. & Bell, M.A. (1986). Historical and ecological
739 sources of variation among lake populations of threespine sticklebacks, Gasterosteus
740 aculeatus, near Cook Inlet, Alaska. *Canad J Zool*, 64, 2257-2265.
741 Gautier, M., Gharbi, K., Cezard, T., Foucaud, J., Kerdelhue, C., Pudlo, P. *et al.* (2013). The
742 effect of RAD allele dropout on the estimation of genetic variation within and between
743 populations. *Mol Ecol*, 22, 3165-3178.
744 Glazer, A.M., Killingbeck, E.E., Mitros, T., Rokhsar, D.S. & Miller, C.T. (2015). Genome
745 Assembly Improvement and Mapping Convergently Evolved Skeletal Traits in
746 Sticklebacks with Genotyping-by-Sequencing. *G3-Genes Genom Genet*, 5, 1463-1472.
747 Grant, P.R. & Grant, B.R. (2002). Unpredictable evolution in a 30-year study of Darwin's finches.
748 *Science*, 296, 707-711.
749 Guerrero, R.F., Rousset, F. & Kirkpatrick, M. (2012). Coalescent patterns for chromosomal
750 inversions in divergent populations. *Philos Trans Roy Soc B*, 367, 430-438.
751 Hendry, A.P., Taylor, E.B. & McPhail, J.D. (2002). Adaptive divergence and the balance
752 between selection and gene flow: lake and stream stickleback in the Misty system.
753 *Evolution*, 56, 1199-1216.
754 Hohenlohe, P.A., Bassham, S., Etter, P.D., Stiffler, N., Johnson, E.A. & Cresko, W.A. (2010).
755 Population genomics of parallel adaptation in threespine stickleback using sequenced
756 RAD tags. *Plos Genet*, 6, e1000862.
757 Hudson, R.R., Slatkin, M. & Maddison, W.P. (1992). Estimation of Levels of Gene Flow from
758 DNA-Sequence Data. *Genetics*, 132, 583-589.

759 Huerta-Sánchez, E., Jin, X., Asan, Bianba, Z., Peter, B.M., Vinckenbosch, N. *et al.* (2014).
760 Altitude adaptation in Tibetans caused by introgression of Denisovan-like DNA. *Nature*,
761 512, 194-197.
762 Jones, F.C., Grabherr, M.G., Chan, Y.F., Russell, P., Mauceli, E., Johnson, J. *et al.* (2012). The
763 genomic basis of adaptive evolution in threespine sticklebacks. *Nature*, 484, 55-61.
764 Kimmel, C.B., Ullmann, B., Walker, C., Wilson, C., Currey, M., Phillips, P.C. *et al.* (2005).
765 Evolution and development of facial bone morphology in threespine sticklebacks. *Proc*
766 *Natl Acad Sci U S A*, 102, 5791-5796.
767 Kingman, J.F.C. (1982a). The coalescent. *Stoch Proc Appl*, 13, 235-248.
768 Kingman, J.F.C. (1982b). On the genealogy of large populations. *J Appl Probab*, 19, 27-43.
769 Kirkpatrick, M. & Barton, N. (2006). Chromosome inversions, local adaptation and speciation.
770 *Genetics*, 173, 419-434.
771 Lenormand, T. (2002). Gene flow and the limits to natural selection. *TREE,* 17, 183-189.
772 Lescak, E.A., Bassham, S.L., Catchen, J., Gelmond, O., Sherbick, M.L., von Hippel, F.A. *et al.*
773 (2015). Evolution of stickleback in 50 years on earthquake-uplifted islands. *Proc Natl*
774 *Acad Sci U S A*, 112, E7204-7212.
775 Li, H., Handsaker, B., Wysoker, A., Fennell, T., Ruan, J., Homer, N. *et al.* (2009). The Sequence
776 alignment/map (SAM) format and SAMtools. *Bioinformatics*, 25, 2078-2079.
777 Linnen, C.R., Kingsley, E.P., Jensen, J.D. & Hoekstra, H.E. (2009). On the origin and spread of
778 an adaptive allele in deer mice. *Science*, 325, 1095-1098.
779 McCairns, R.J.S. & Bernatchez, L. (2012). Plasticity and heritability of morphological variation
780 within and between parapatric stickleback demes. *J Evol Biol*, 25, 1097-1112.
781 McGuigan, K., Nishimura, N., Currey, M., Hurwit, D. & Cresko, W.A. (2011). Cryptic genetic
782 variation and body size evolution in threespine stickleback. *Evolution*, 65, 1203-1211.
783 McKinnon, J.S. & Rundle, H.D. (2002). Speciation in nature:the threespine stickleback model
784 systems. *TREE*, 17, 480-488.
785 Miller, C.T., Glazer, A.M., Summers, B.R., Blackman, B.K., Norman, A.R., Shapiro, M.D. *et al.*
786 (2014). Modular Skeletal Evolution in Sticklebacks Is Controlled by Additive and
787 Clustered Quantitative Trait Loci. *Genetics*, 197, 405-420.
788 Nei, M. (1987). *Molecular evolutionary genetics*. Columbia university press.
789 Ormond, L., Foll, M., Ewing, G.B., Pfeifer, S.P. & Jensen, J.D. (2016). Inferring the age of a
790 fixed beneficial allele. *Mol Ecol*, 25, 157-169.
791 Orr, H.A. (2005). The genetic theory of adaptation: a brief history. *Nat Rev Genet*, 6, 119-127.
792 Otto, S.P. & Bourguet, D. (1999). Balanced polymorphisms and the evolution of dominance. *Am*
793 *Nat*, 153, 561-574.
794 Paradis, E. (2010). pegas: an R package for population genetics with an integrated-modular
795 approach. *Bioinformatics*, 26, 419-420.
796 Paradis, E., Claude, J. & Strimmer, K. (2004). APE: Analyses of Phylogenetics and Evolution in
797 R language. *Bioinformatics*, 20, 289-290.
798 Pease, J.B., Haak, D.C., Hahn, M.W. & Moyle, L.C. (2016). Phylogenomics reveals three
799 sources of adaptive variation during a rapid radiation. *PLoS Biol*, 14, e1002379.
800 Peter, B.M., Huerta-Sanchez, E. & Nielsen, R. (2012). Distinguishing between Selective
801 Sweeps from Standing Variation and from a De Novo Mutation. *Plos Genet*, 8.
802 Peterson, B.K., Weber, J.N., Kay, E.H., Fisher, H.S. & Hoekstra, H.E. (2012). Double Digest
803 RADseq: An Inexpensive Method for De Novo SNP Discovery and Genotyping in Model
804 and Non-Model Species. *Plos One*, 7.
805 Pfeifer, B., Wittelsburger, U., Ramos-Onsins, S.E. & Lercher, M.J. (2014). PopGenome: An
806 Efficient Swiss Army Knife for Population Genomic Analyses in R. *Mol Biol Evol*, 31,
807 1929-1936.

Phillips, P.C. (2008). Epistasis--the essential role of gene interactions in the structure and evolution of genetic systems. *Nat Rev Genet*, 9, 855-867.

Popescu, A.A., Huber, K.T. & Paradis, E. (2012). ape 3.0: New tools for distance-based phylogenetics and evolutionary analysis in R. *Bioinformatics*, 28, 1536-1537.

Reimchen, T.E. (1994). Predators and morphological evolution in threespine stickleback. In: *The Evolutionary Biology of the Threespine Stickleback* (eds. Bell, MA & Foster, SA). Oxford University Press New York, pp. 240-276.

Roesti, M., Gavrilets, S., Hendry, A.P., Salzburger, W. & Berner, D. (2014). The genomic signature of parallel adaptation from shared genetic variation. *Mol Ecol*, 23, 3944-3956.

Roesti, M., Kueng, B., Moser, D. & Berner, D. (2015). The genomics of ecological vicariance in threespine stickleback fish. *Nat Commun*, 6, 8767.

Roesti, M., Moser, D. & Berner, D. (2013). Recombination in the threespine stickleback genome - Patterns and consequences. *Mol Ecol*, 22, 3014-3027.

Samuk, K., Owens, G.L., Delmore, K.E., Miller, S., Rennison, D.J. & Schluter, D. (2017). Gene flow and selection interact to promote adaptive divergence in regions of low recombination. *Mol Ecol*, 26, 4378-4390.

Schlotterer, C., Tobler, R., Kofler, R. & Nolte, V. (2014). Sequencing pools of individuals-mining genome-wide polymorphism data without big funding. *Nat Rev Genet*, 15, 749-763.

Schluter, D. & Conte, G.L. (2009). Genetics and ecological speciation. *Proc Natl Acad Sci U S A*, 106 Suppl 1, 9955-9962.

Schrider, D.R. & Kern, A.D. (2017). Soft Sweeps Are the Dominant Mode of Adaptation in the Human Genome. *Mol Biol Evol*, 34, 1863-1877.

Stankowski, S. & Streisfeld, M.A. (2015). Introgressive hybridization facilitates adaptive divergence in a recent radiation of monkeyflowers. *Proc Roy Soc B-Biol Sci*, 282, 20151666.

Stephens, M. & Scheet, P. (2005). Accounting for decay of linkage disequilibrium in haplotype inference and missing-data imputation. *Am J Hum Genet*, 76, 449-462.

Stephens, M., Smith, N.J. & Donnelly, P. (2001). A new statistical method for haplotype reconstruction from population data. *Am J Hum Genet*, 68, 978-989.

Stuart, Y.E., Veen, T., Weber, J.N., Hanson, D., Ravinet, M., Lohman, B.K. *et al.* (2017). Contrasting effects of environment and genetics generate a continuum of parallel evolution. *Nat Ecol Evol*, 1, 0158.

Tajima, F. (1983). Evolutionary Relationship of DNA-Sequences in Finite Populations. *Genetics*, 105, 437-460.

R Core Team. (2016). R: A language and environment for statistical computing. R Foundation for Statistical Computing Vienna, Austria.

Wakeley, J. (2009). *Coalescent Theory: An Introduction*. Harvard University.

Willing, E.M., Dreyer, C. & van Oosterhout, C. (2012). Estimates of Genetic Differentiation Measured by F-ST Do Not Necessarily Require Large Sample Sizes When Using Many SNP Markers. *Plos One*, 7.

Wright, K.M., Lloyd, D., Lowry, D.B., Macnair, M.R. & Willis, J.H. (2013). Indirect Evolution of Hybrid Lethality Due to Linkage with Selected Locus in Mimulus guttatus. *PLoS Biol*, 11.

Wright, S. (1932). The roles of mutation, inbreeding, crossbreeding and selection in evolution. *Proceedings of the Sixth International Congress on Genetics*, 1, 356-366.

Wund, M.A., Singh, O.D., Geiselman, A. & Bell, M.A. (2016). Morphological evolution of an anadromous threespine stickleback population within one generation after reintroduction to Cheney Lake, Alaska. *Evol Ecol Res*, 17, 203-224.

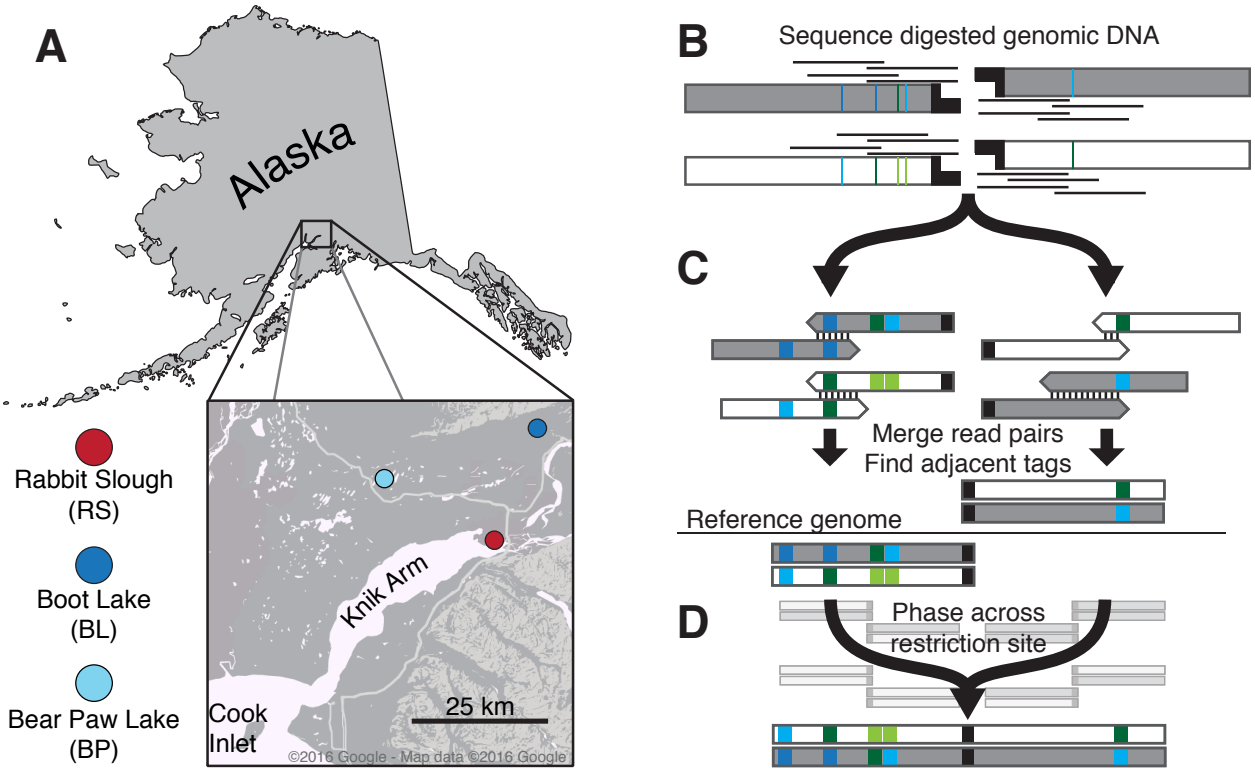

Figure 1. Stickleback sampling and RAD sequencing to measure haplotype variation. A) Threespine stickleback sampling locations in this study. Colors represent habitat type: red: marine; blue: freshwater. B-D: We modified the original RAD-seq protocol to generate local haplotypes. Colored bars represent polymorphic sites. For a detailed description of haplotype construction, see *Methods*. B) Overlapping paired-end reads are anchored to *PstI* restriction sites. C) Paired reads mapping to each halfsite are merged into contigs. Contigs mapping to the same restriction site are identified by alignment to the reference genome. D) Sequences from each half of a restriction site are phased to generate a single RAD locus. RAD tags in the background represent multiple genotypes used in phasing.

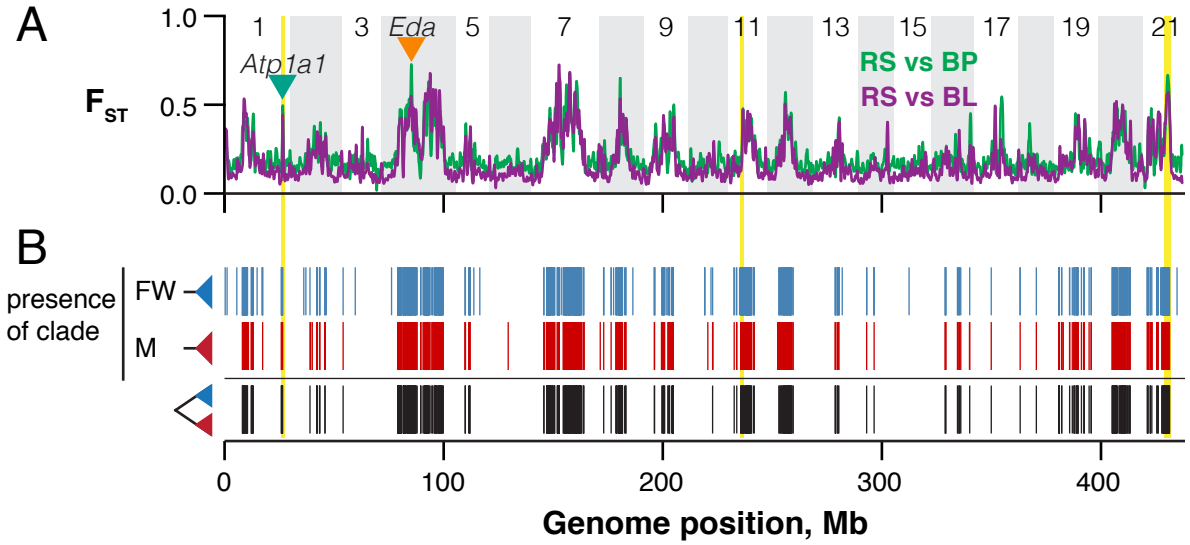

Figure 2. The genealogical structure of parallel genomic divergence. A) Genome-wide F_{ST} for both marine-freshwater comparisons was kernel-smoothed using a normally distributed kernel with a window size of 500 kb. Inverted triangles indicate the locations of two genes known to show extensive marine-freshwater haplotype divergence, *Eda* and *Atp1a1*. Three chromosomal inversions are highlighted in yellow. B) Lineage sorting patterns were identified from maximum clade credibility trees for each RAD locus. Blue bars: haplotypes from both freshwater populations form a single monophyletic group; red: haplotypes from the marine population form a monophyletic group; black: A RAD locus is structured into reciprocally monophyletic marine and freshwater haplogroups.

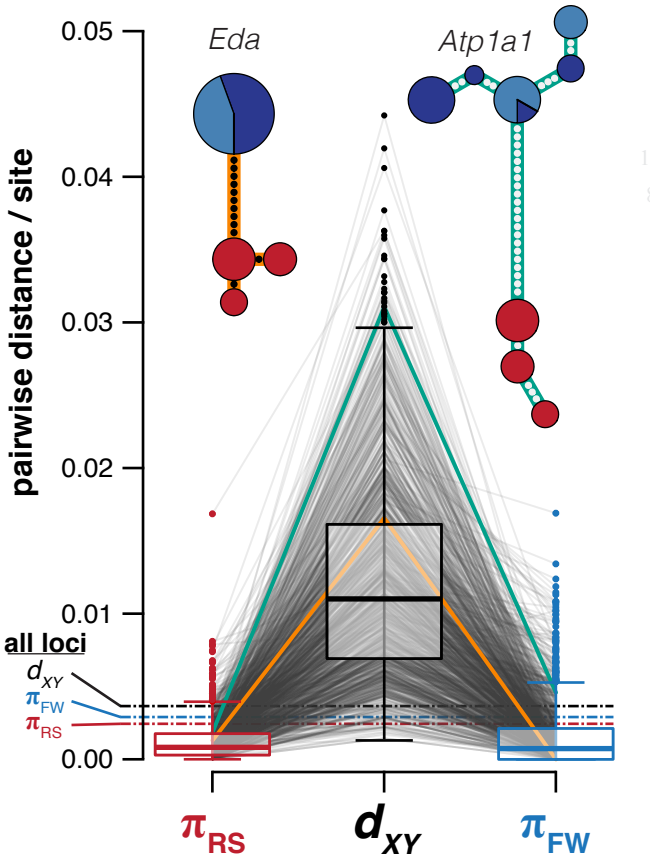

Figure 3. Extensive sequence divergence between marine and freshwater haplogroups accompanies reciprocal monophyly. For each reciprocally monophyletic RAD locus, we calculated sequence variation (π) within and sequence divergence between habitat types (d_{XY}). Each RAD locus is shown as a pair of lines connecting estimates of π and d_{XY}. Boxplots show distributions across all reciprocally monophyletic RAD loci: Boxes are upper and lower quartiles, including the median; whiskers extend to 1.5x interquartile range. Dashed lines are the genome-wide medians. Single RAD loci from within the transcribed regions of *Eda* and *Atp1a1* are shown as gold and green lines, respectively, and presented as haplotype networks. Dots represent mutational steps. Circle sizes indicate the number of haplotypes and colors indicate population of origin as in Figure 1. Each network = 29 haplotypes.

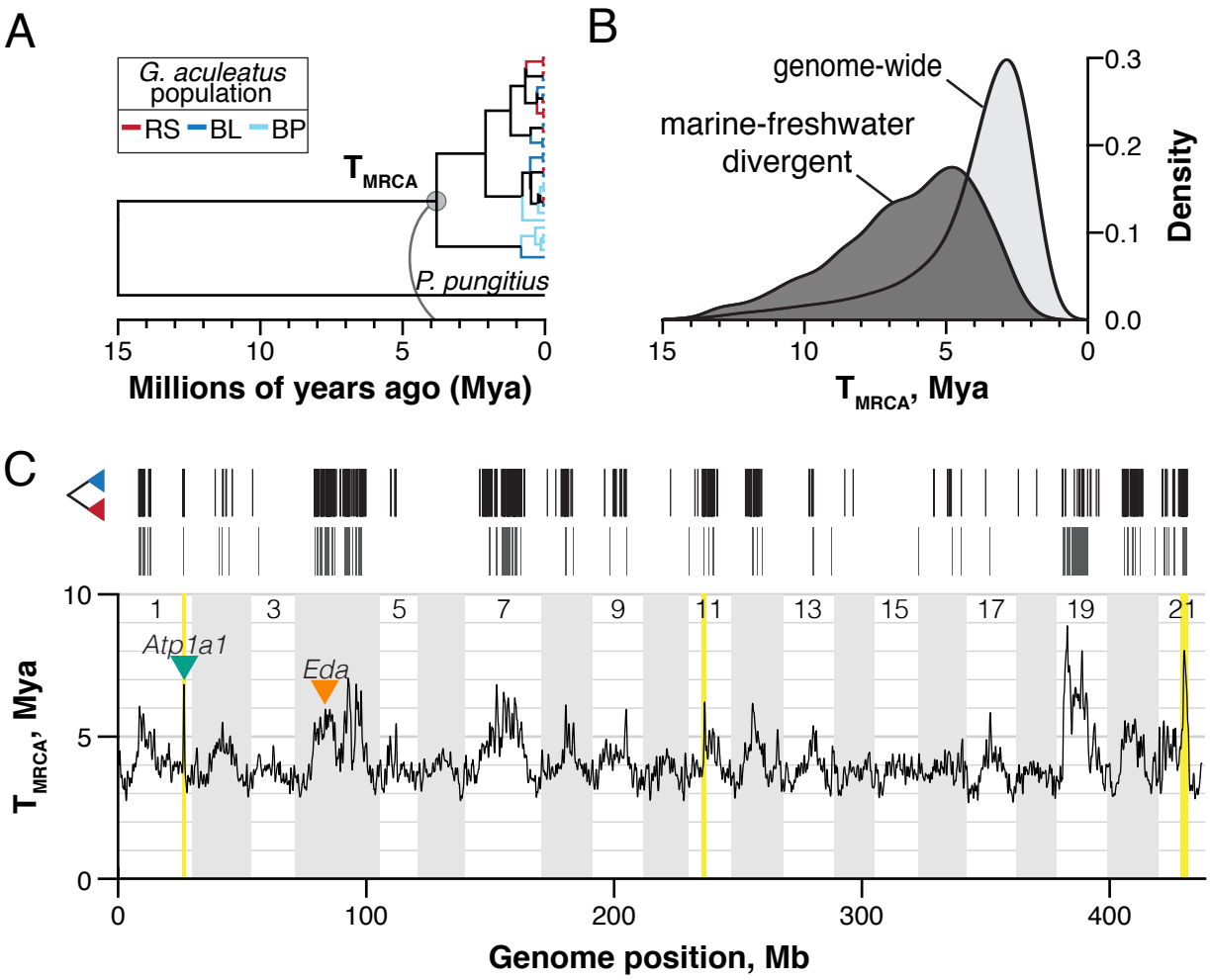

Figure 4. Marine-freshwater divergence has evolved over millions of years, affecting large genomic regions. We performed Bayesian estimation of the time to the most recent common ancestor (T_{MRCA}) of alleles at threespine stickleback RAD loci. We calibrated coalescence times within threespine stickleback by including a *de novo* genome assembly from the ninespine stickleback (*Pungitius pungitius*) and setting threespine-ninespine divergence at 15 million years ago. A) Maximum clade credibility RAD gene tree representative of the genome-wide average T_{MRCA}. Branches within threespine are colored by population of origin. B) Kernel-smoothed densities of T_{MRCA} distributions for all RAD loci containing a monophyletic group of threespine stickleback alleles (light gray) and those structured into reciprocally monophyletic marine and freshwater haplogroups. C) The genomic distribution of reciprocally monophyletic RAD loci (black, as in Figure 2) is associated with increased T_{MRCA} at a genomic scale. T_{MRCA} outlier windows (those exceeding 99.9% of permuted genomic windows) are shown as gray bars. Genome-wide T_{MRCA} was kernel-smoothed using a normally distributed kernel with a window size of 500 kb. Inverted triangles indicate the locations of *Eda* and *Atp1a1*. Three chromosomal inversions are highlighted in yellow.

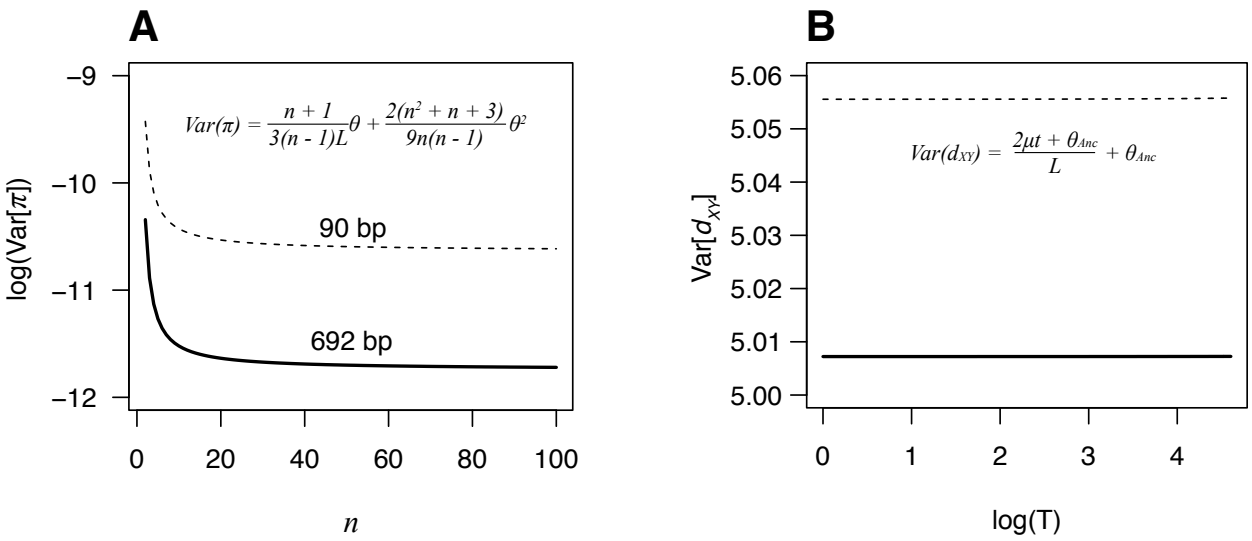

Figure S1. Longer sequences reduce variance in estimates of sequence diversity and divergence. A: Variance in π as a function of the number of chromosomes sampled, using sequence lengths typical of RAD-seq experiments (90 bp) and those in this study (692 bp). Variance was calculated using equation 10.9 in Nei (1987). Right: Variance in d_{XY} (using the equation in box 1 in Cruickshank and Hahn (2014)) as a function of (log-scaled) divergence time of two populations. The change in variance as function of divergence time is dwarfed by the difference in variance obtained with different sequence lengths. In both panels, n = sequences sampled; L = length of sequence sampled; $\theta = 4N\mu$; $\theta_{Anc} = \theta$ in the population ancestral to those sampled; μ = mutation rate per nucleotide; t = time since population split.

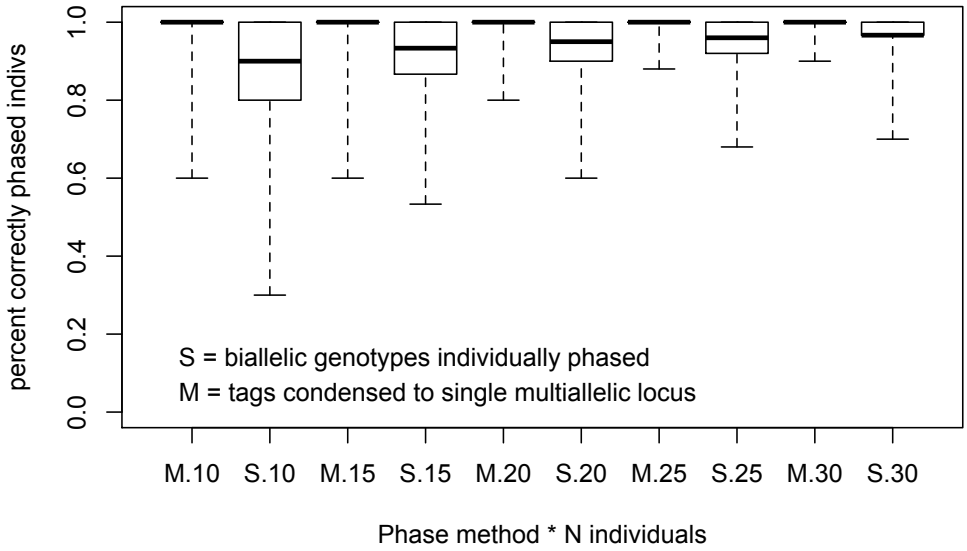

Figure S2. Accurate phasing of RAD loci even at low population-level sampling. Neutrally evolving, non-recombining RAD loci were simulated with ms and seq-gen to generate alignments with of 20 to 60 haplotypes (10-30 diploid individuals) and four to 30 segregating sites. Simulated haplotypes were then 'cut' at their midpoints and phased either by inputting all variable sites individually (biallelic 'SNPs', S) or by inputting the haplotype information on either site of the cut as multiallelic loci (M). Boxes represent interquartile range (IQR). Bold lines are medians. Whiskers extend to minimum and maximum values. Even with smaller sample sizes (10-15 individuals), over 75% of phasing attempts resulted in 100% phasing accuracy.

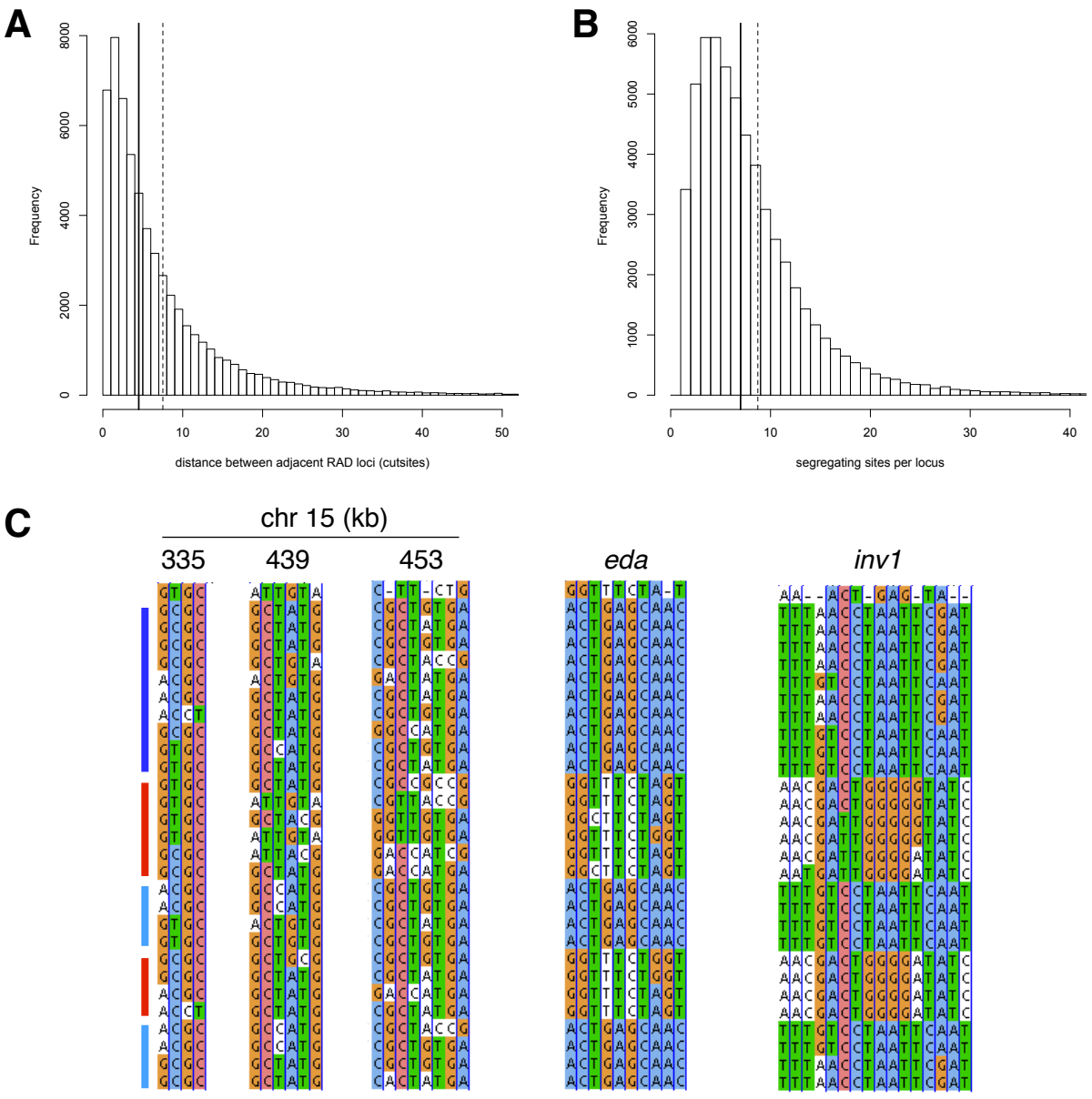

Supplementary Figure S3. RAD-seq effectively samples genome-wide sequence diversity. Histograms of (A) the distance between adjacent RAD loci (calculated as the distance between the centers of each restriction site) and (B) the number of variable sites per locus show that most RAD loci were within 4 kb of their nearest neighbor and contained ≥ 7 variable sites. Means for each metric are shown as dashed vertical lines. Medians are solid lines. Each histogram is truncated to highlight the bulk of the distribution. Maximum values: distance = 455 kb; variable sites = 155. C: Example haplotypes from five RAD loci in non-divergent (chromosome 15) and divergent (*eda*, *inv1*) genomic regions. Chromosome 15 loci are labeled by their genomic position. The *eda* RAD locus is within the transcribed region of *eda* and *inv1* is within the breakpoints of the chromosome 1 inversion. Colored bars identify population/ecotype of origin. Red: RS (marine); dark blue: BL (freshwater); light blue: BP (freshwater). Alignments visualized in JalView v1.0 (Waterhouse, *et al*, 2009). Only sites that are variable within threespine stickleback are shown.

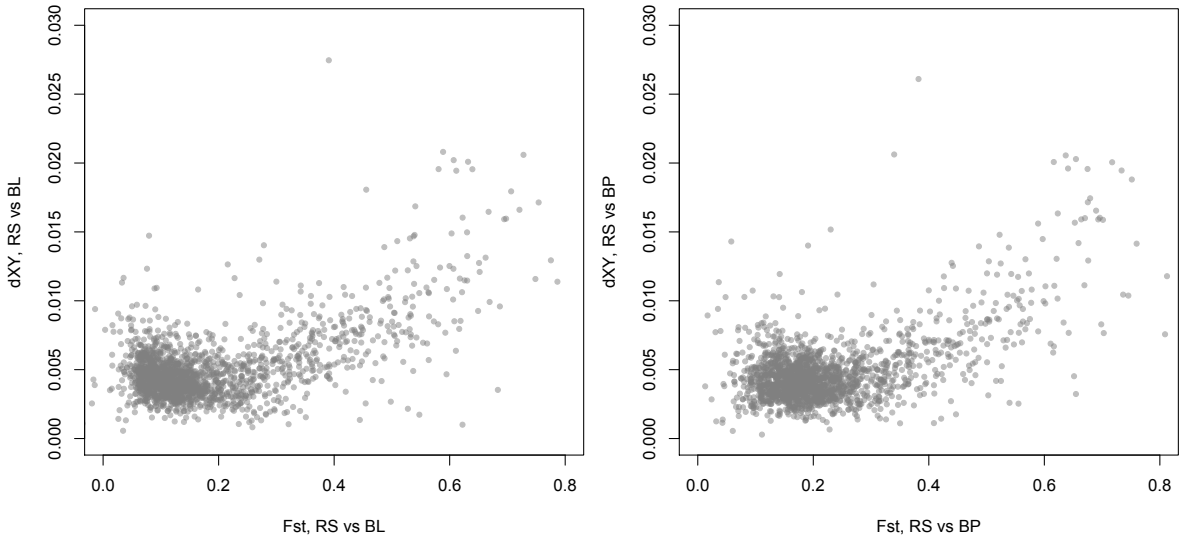

Supplementary Figure S4. Relative (F_{ST}) and absolute (d_{XY}) sequence divergence are positively correlated genome-wide in two instances of marine-freshwater divergence. Points are 250 kb non-overlapping genomic windows. Left panel compares the marine Rabbit Slough population (RS) to the freshwater Boot Lake population (BL) (type-II linear model: $r^2 = 0.314$, permuted p-value [reduced major axis] = 0.01). Right panel compares RS to the freshwater Bear Paw Lake population (BL) (type-II linear model: $r^2 = 0.311$, permuted p-value [reduced major axis] = 0.01).

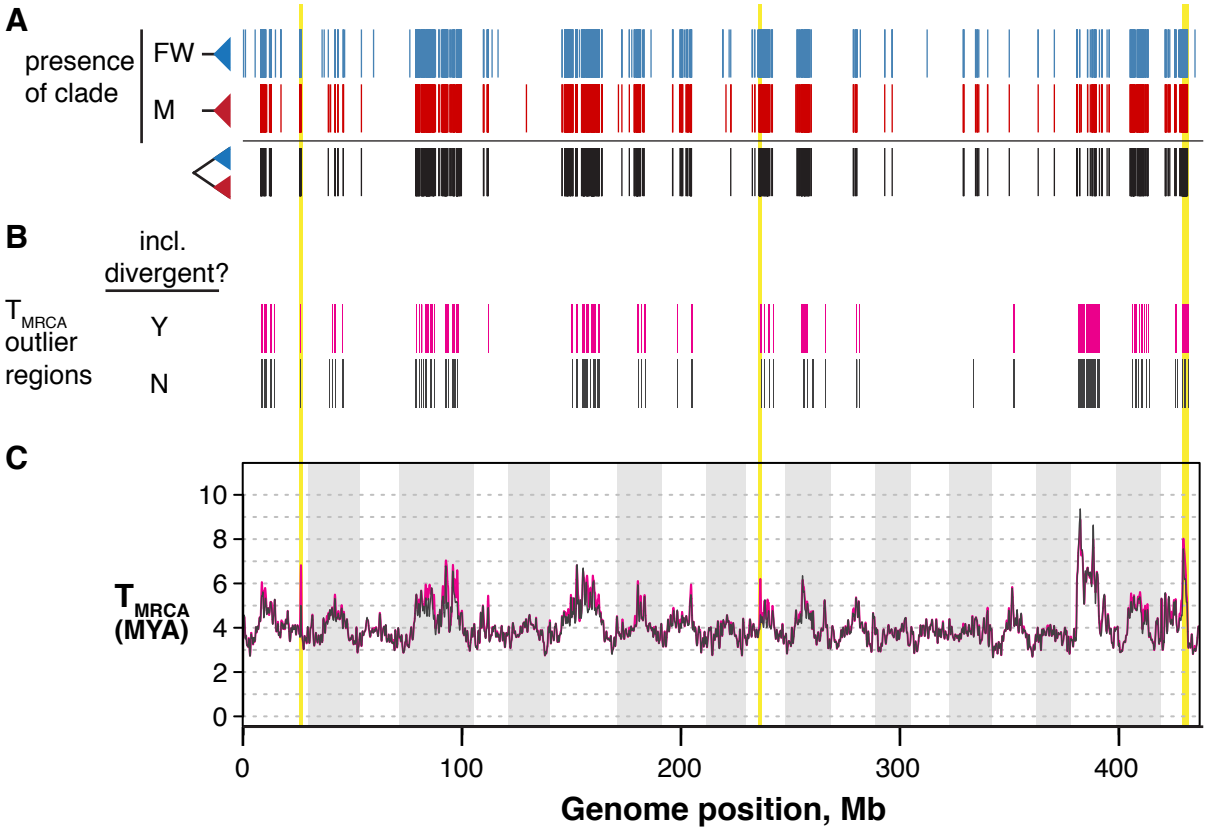

Supplementary Figure S5. T_{MRCA} outlier regions remain outliers after removing highly differentiated RAD loci. Panel A is taken from Fig. 2 and shows the genomic distribution of reciprocally monophyletic ("divergent"; black bars) RAD loci. Panel B shows the distributions of T_{MRCA} outlier regions (increased T_{MRCA}) including all RAD loci (magenta boxes, "Y"). Below are the T_{MRCA} outlier regions after removing divergent loci and any RAD locus with a marine-freshwater (RS vs. [BL+BP]) $F_{ST} > 0.5$, which is approximately the top 7% of the F_{ST} distribution. Panel C: Genome scans of T_{MRCA} using all RAD loci (magenta) and excluding marine-freshwater outliers (gray).

Supplementary table 1. Sequencing summary for threespine stickleback samples

Sample	population	raw reads	filtered reads	merged pairs	mean coverage per locus
1827.05	Rabbit Slough	10167407	10031967	7269377	12X
1827.06	Rabbit Slough	10265078	10172621	7591801	13X
1827.07	Rabbit Slough	9175983	9040625	6771332	11X
1827.08	Rabbit Slough	7896938	7814081	5879351	10X
1827.09	Rabbit Slough	8773502	8668261	6405777	11X
2827.01	Boot Lake	8917575	8810382	6373001	11X
2827.07	Boot Lake	10064876	9917732	7255989	13X
2827.13	Boot Lake	9099831	9002717	6528704	12X
2827.19	Boot Lake	11021084	10792092	7911026	14X
2827.25	Boot Lake	9920574	9814758	7287485	13X
1902.02	Bear Paw Lake	4780489	4365505	2942926	5X
1902.03	Bear Paw Lake	5073434	4643909	3192582	5X
1902.04	Bear Paw Lake	4902931	4600877	3138791	6X
1902.06	Bear Paw Lake	4501906	4339253	2983345	5X

Supplementary table 2. Genome assembly statistics for *Pungitius pungitius*.

	contig (scaffold)
n	393,037 (391,396)
Max length (bp)	165,088 (182,644)
N50 (bp)	9,202 (9,886)
Average length (bp)	1,314 (1,320)
Gaps (%)	0.03
Total assembly length (bp)	516,674,741